Universiteit Antwerpen

This item is the archived peer-reviewed author-version of:

Research on the self-healing behavior of asphalt mixed with healing agents based on molecular dynamics method

Reference:
He Liang, Zheng Yufeng, Alexiadis Alessio, Falchetto Augusto Cannone, Li Guannan, Valentin Jan, Van den bergh Wim, Vasiliev Yuri Emmanuilovich, Kowalski Karol J., Grenfell James.- Research on the self-healing behavior of asphalt mixed with healing agents based on molecular dynamics method
Construction and building materials - ISSN 0950-0618 - 295(2021), 123430
Full text (Publisher's DOI): https://doi.org/10.1016/J.CONBUILDMAT.2021.123430
To cite this reference: https://hdl.handle.net/10067/1797420151162165141

uantwerpen.be
Institutional repository IRUA

Research on the self-healing behavior of asphalt mixed with healing agents based on molecular dynamics method

Liang He[*a], Yufeng Zheng[b], Alessio Alexiadis[c], Augusto Cannone Falchetto[d], Guannan Li[e], Jan Valentin[f], Wim Van den bergh[g], Yuri Emmanuilovich Vasiliev[h], Karol J Kowalski[i], James Grenfell[j]

[a] *State Key Laboratory of Mountain Bridge and Tunnel Engineering, Chongqing Jiaotong University, Chongqing 400074, China*

[b] *Chongqing Jiaduo Highway Design Consulting Co. , Ltd., Chongqing 400000, China*

[c] *School of Chemical Engineering, University of Birmingham, Birmingham B15 2TT, United Kingdom*

[d] *Department of Civil Engineering, Aalto University, Espoo 02150, Finland*

[e] *School of Transportation Science and Engineering, Harbin Institute of Technology, Harbin 150090, Heilongjiang, China*

[f] *Faculty of Civil Engineering, Czech Technical University in Prague, 166 29 Prague 6, Czech Republic*

[g] *Faculty of Applied Engineering, University of Antwerp, Antwerp G.Z.352, Belgium*

[h] *Department of Road Building Materials, Moscow Automobile and Road State Technical University, Moscow 125319, Russian Federation*

[i] *Faculty of Civil Engineering, Warsaw University of Technology, Warsaw 00-637, Poland*

[j] *ARRB, 80a Turner St, Port Melbourne, VIC 3207, Australia*

Highlights

> A model of asphalt microcrack containing healing agents is established.

> A short-term aged asphalt model is established.

> Models of plant oil and aromatic oil as typical healing agents are established.

> A method for analyzing asphalt self-healing rate by diffusion coefficient is proposed.

ABSTRACT

Molecular dynamics is used to simulate the self-healing process of asphalts mixed with a healing agent. Sulfoxide functional groups were introduced into the virgin asphalt to produce a short-term-aged asphalt model. The model is validated by comparing density, diffusion coefficient, solubility parameter, and viscosity with real measurements. Plant oil and Aromatic oil are chosen as typical healing agents. The molecular models of asphalt and healing agent are integrated into a micro-crack model, and the healing process is simulated with molecular dynamics.

*Corresponding author.

E-mail addresses: lianghe@cqjtu.edu.cn(L.He)

The results show that Plant oil is a better choice for improving the healing rate of virgin asphalt, while Aromatic oil is better for improving the healing rate of short-term-aged asphalt. The higher the temperature is, the better effect the healing agent will have on the asphalt. Healing is maximized above 15 □ for virgin asphalt and above 45 □ for short-term-aged asphalt. Molecular simulations show that the healing process depends on the diffusion of the healing agent and asphalt into the micro-crack. After the crack is filled, bitumen and oil molecules continue to mix. Aromatic oil produces a better mixing that leads to a more uniform composition and better mechanical properties.

Keywords： Asphalt; Molecular dynamics; Self-healing; Healing agent; Short-term aged

1 Introduction

Asphalt is a type of binder with an extremely complex chemical composition that is widely used in the construction and maintenance of high-grade highways. The effect of traffic, oxygen, UV radiation, thermal cycling, and ambient moisture results in the formation of microcracks in the asphalt mixture. This process is naturally mitigated by the drainage of bitumen into the microcracks, which effectively "self-heals" the road surface [1]. However, bitumen is highly viscous at ambient temperature. Thus, self-healing is slow, and the rate of crack growth can be faster than the healing process. To improve self-healing, plant oil [3][4], aromatic oil [5], or light oil [6] can be added to the mixture. This softens the asphalt, activates the crack surface, and accelerates drainage of bitumen into the microcracks. These oils can be stored in microcapsules and mixed into the bitumen. In this way, capsules remain intact until the crack occurs, and the healing agent is released only when it is needed.

Macroscopic tests show that the healing agent plays an active role in the self-healing of asphalt; however, they cannot explain this mechanism at the molecular level. Many researchers have used molecular dynamics (MD) to investigate the molecular properties of asphalt. According to the component classification, the asphalt model can be divided into three-components [7] and four-components [8]. At present, the models of virgin asphalt, aged asphalt [9-13], SBS-modified asphalt [14], and rubber modified asphalt models [15][16] are mostly derived from the four-component asphalt model. Moreover, the virgin asphalt model can be mixed with modifier molecules to set up foamed-asphalt [17], recycled-asphalt [10], and asphalt-interface models [18]. Bhasin and Greenfield [19] used MD to simulate the self-healing process of asphalt designing a micro-crack model of asphalt under vacuum. Sun et al. [20] used the three-components asphalt model for simulating the healing of a 10Å micro-crack and measured the diffusion coefficient, activation energy, and the former index factor. Sun [21] used the virgin four-component model and a 20Å crack to simulate the self-repair process of asphalt at different temperatures. The optimal repair temperature was found between 40□ and 49□. Xu [22] used a four-components model, to simulate self-healing of both virgin and aged asphalt and found that the self-repair effect of the aged-asphalt is significantly lower.

At present, research on asphalt healing is limited to virgin, aged, and SBS-modified asphalt. Self-healing of asphalt mixed with healing agents has not been investigated thoroughly and deserves further study. Although many experiments have confirmed that healing agents improve self-healing, the performance of different agents is normally not compared. Moreover, the microscopic mechanism of self-healing of asphalt mixed with the healing agents is still not clear. This paper compares two typical healing agents (plant oil and aromatic oil). Self-healing is simulated with MD and the effects of the different agents compared.

2 MD Simulation models and methods

2.1 Virgin and short-aged asphalt MD models

In this paper, we choose the four-components virgin asphalt model with twelve molecules AAA-1 designed by Greenfield's team [8]. The molecular structure of some of the molecules is adjusted according to Petersen's asphalt-aging theory [23-27] (asphalt mainly forms sulfoxide functional groups in the short-term aging stage and ketone functional groups in the long-term aging stage). Additionally, the content of asphaltene in the virgin asphalt model is slightly increased, while the content of aromatic fraction, saturated fraction, and resin fraction is slightly decreased to reflect experimental data of the content of the four components in the short-term aged asphalt [28-30]. Finally, the number of molecules of each type is adjusted according to the content of the four components. The total atomic mass of the virgin asphalt model is 32694 Da, while the total atomic mass of the short-term aged asphalt model is 32549 Da. The molecular structure is shown in fig.1, and the molecular composition in Table 1.

Table 1 Molecular composition of virgin and short-term aged asphalt model(AAA-1).

Fraction	Molecules	Molecular formula	Molecular weight [Da]	Virgin asphalt		Short-term aged asphalt	
				Number of molecules	Fraction Content [%]	Number of molecules	Fraction Content [%]
Asphaltene	Asphaltene-A	$C_{42}H_{54}O$	575.0	3	17.28	4	24.14
	Asphaltene-B	$C_{66}H_{81}N$	888.5	2		3	
	Asphaltene-C	$C_{51}H_{62}S$	707.2	3		0	
	Asphaltene-C1	$C_{51}H_{62}SO$	723.1	0		4	
Saturate	Saturate-A	$C_{30}H_{62}$	422.9	4	11.13	4	9.64
	Saturate-B	$C_{35}H_{62}$	483.0	4		3	
Aromatic	Aromatic-A	$C_{35}H_{44}$	464.8	11	31.95	10	29.27
	Aromatic-B	$C_{30}H_{46}$	406.8	13		12	
Resin	Resin-A	$C_{40}H_{59}N$	554.0	4	39.64	3	36.95
	Resin-B	$C_{40}H_{60}S$	573.1	4		0	
	Resin-B1	$C_{40}H_{60}SO$	589	0		4	
	Resin-C	$C_{18}H_{10}S_2$	290.4	15		0	
	Resin-C1	$C_{18}H_{10}S_2O_2$	322.4	0		15	
	Resin-D	$C_{36}H_{57}N$	530.9	4		3	
	Resin-E	$C_{29}H_{50}O$	414.8	5		4	

The following steps are taken to build virgin and short-term aged asphalt models:

1. Molecules are drawn according to their molecular structure and built in a system box with periodic boundary conditions with an initial density of 0.1g/cm^3.
2. The structure is optimized by minimizing the energy of the initial system box.
3. A MD simulation with a duration of 300ps is carried out in the isothermal-isasteric ensemble (NVT) ensemble.
4. Five cycles of annealing are carried out, the temperature range of annealing is 300K to 500K.
5. Relaxation for a duration of 300ps is carried out in the isothermal-isobaric ensemble (NPT) ensemble.

The final conformation, after these five steps, is shown in fig.2. The box size of the virgin-asphalt model is 38.02×38.02×38.02 (A^3), and the box size of the short-term-aged model is 37.52×37.52×37.52 (A^3).

The virgin asphalt model is simulated for 200ps under the NPT ensemble at 298.15 K. The model is validated by comparing the calculated values of the (i) density, (ii) solubility parameter, (iii) diffusion coefficient, and (iv) viscosity with experimental data. The solubility parameter δ measures the reciprocal solubility of different polymeric liquids, if the solubility parameter of two liquids is similar, they are easily mixed; otherwise, mixing is difficult. It can be calculated as

$$\delta = \sqrt{\frac{E_{\mathrm{coh}}}{V}}, \tag{1}$$

where E_{coh} is the cohesive energy, which refers to the energy required by condensed matter to eliminate the gasification of intermolecular forces, and V is the volume.

The diffusion coefficient provides a measure of the molecular Brownian motion. The mean square displacement (MSD) of asphaltene under the NPT ensemble at 298.15 K is calculated, and the diffusion coefficient D determined according to

$$D = \frac{1}{6}\lim_{t\to+\infty}\frac{d}{dt}\sum_{i=1}^{N}\left\langle \left|r_i(t)-r_i(0)\right|^2\right\rangle, \tag{2}$$

where r is the atomic displacement, $\left\langle \left|r_i(t)-r_i(0)\right|^2\right\rangle$ the MSD，N is the total atomic number, and <... > indicates the average over all the atoms belonging to asphaltene molecules. In eq. (2), D is calculated as t approaches infinity. In practice, simulations can only be run for finite times. Therefore, the diffusion coefficient is approximated as 1/6 of the slope of the MSD versus time curve.

For calculating the viscosity, the asphalt is subjected to a shear of 0.0001ps^{-1} for 200ps in the NVT ensemble, at 533.15 K, with time step 0.2fs. Conformational data are outputted every 1ps, and the stress autocorrelation function is analyzed. Shear Viscosity η can be calculated by [31]

$$\eta = \frac{V}{KT}\int_0^{\infty}\left\langle P_{\alpha\beta}(0)P_{\alpha\beta}(t)\right\rangle dt, \tag{3}$$

where $P_{\alpha\beta}$ is the off-diagonal stress tensor upward of xy, yz and xz, <... > is the ensemble average, V is the volume

of the system, K is the Boltzmann constant, T is temperature.

The calculated properties of virgin and short-term aged asphalt from MD simulations are compared in Table 2. After short-term ageing, density and solubility change little, viscosity increases, and asphaltene diffusion decreases. In general, the values calculated are in good agreement with experimental data. The difference between the calculated diffusion coefficient and the experimental data [32] is probably due to the different environment of asphaltene (asphalt in the experiment is diluted compared to the simulations).

Table 2 Calculated properties of virgin and short-term aged asphalt from MD simulations.

Properties	Calculation (virgin asphalt)	Calculation (short-term aged asphalt)	experimental or simulated data
Density(298.15K,g/cm^3)	1	1.018	1.01-1.04[33]
Solubility parameter(J/cm^3)$^{0.5}$	18.06	18.15	13.30-22.50[34][35]
Asphaltene diffusion coefficient(cm^2/s)	0.26×10^{-6}	0.12×10^{-6}	3.5×10^{-6}[32]
Viscosity (533.15K, cp)	1.76	2.91	2.20[8]

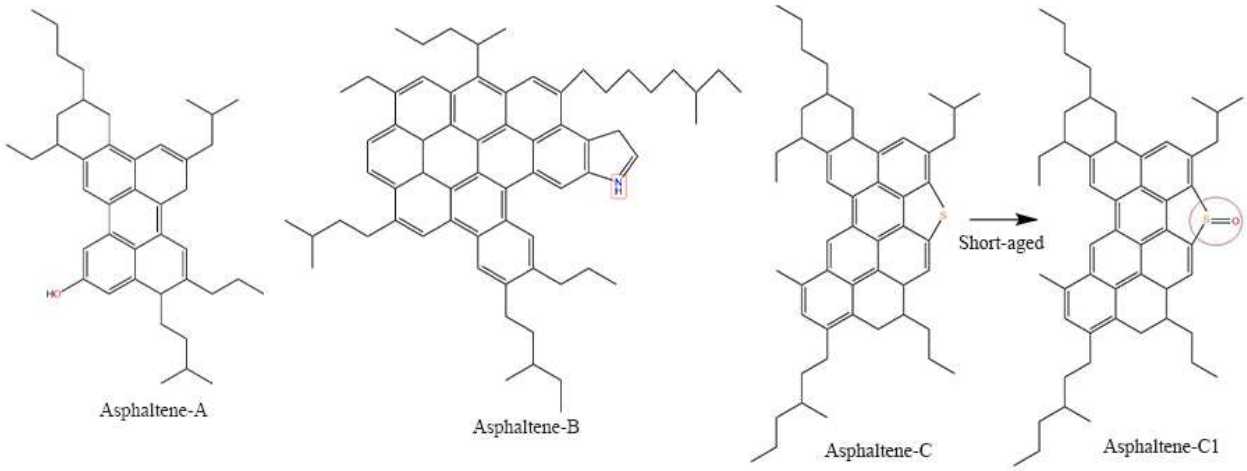

(a) Asphaltene

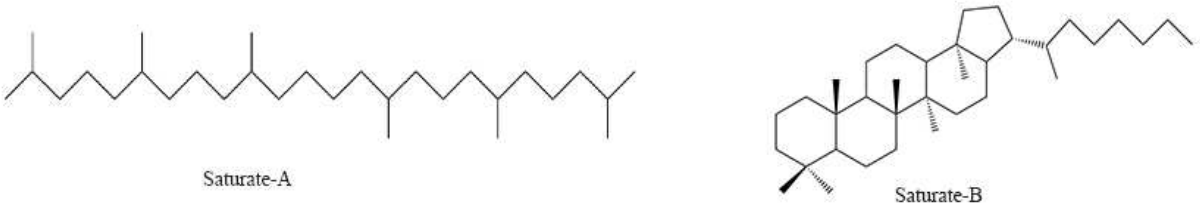

(b) Saturate

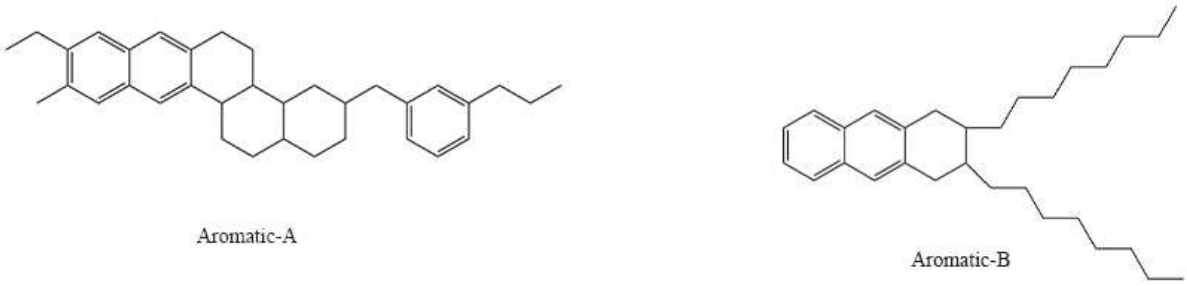

(c) Aromatic

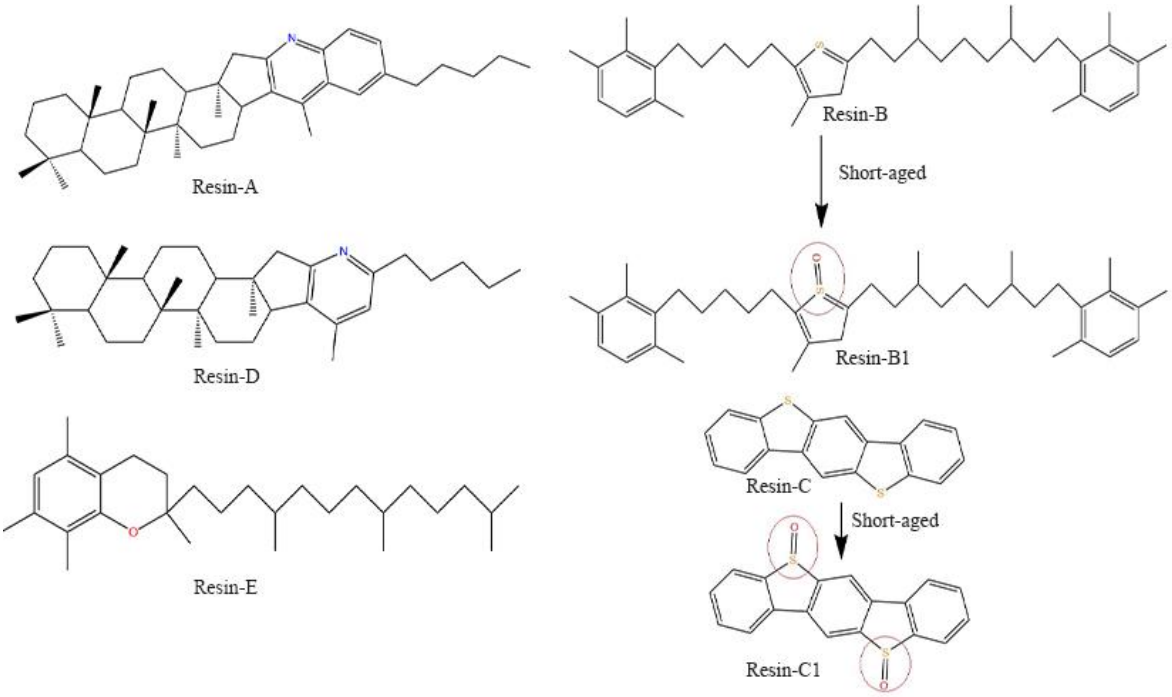

(d) Resin

Fig.1. Molecular structures of virgin and short-aged asphalt

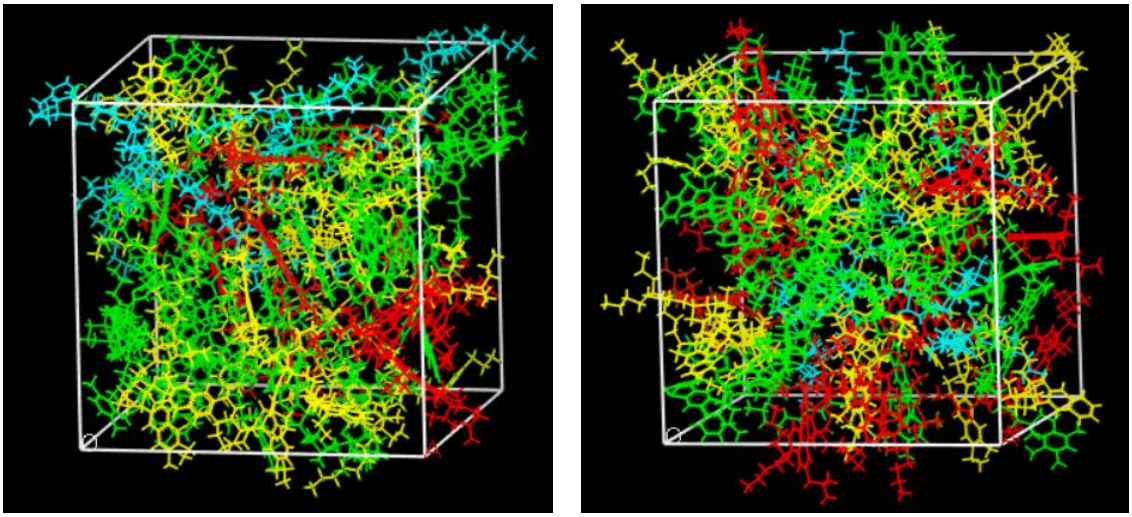

(a) Virgin asphalt (b) Short-term aged asphalt

Fig.2. Virgin and short-term aged asphalt MD model (red: Asphaltene, blue: Saturate, yellow: Aromatic, green: Resin)

2.2 Micro-crack model of asphalt mixed with and without healing agent

In our simulations, we use two common healing agents: Plant oil [3] and Aromatic oil [5]. The main components of the Plant oils are unsaturated fatty acids such as oleic acid, linoleic acid, linolenic acid [36]. The main component of aromatic oils is the aromatic component (e.g. ethyltetralin [10][12]). The molecular structures of the healing agents

are shown in Fig.3, and their molecular composition is shown in Table 3.

To assess the effect of the healing agent, we carry out two simulations under the same conditions: one with the healing agent and one without. In the model, the micro-crack is represented by an empty layer of 20Å in the middle of the simulation box Fig.4(e). We assume that the healing agent is equally distributed on both sides of the crack. The simulations are carried out as follows:

1. the layer of the healing agent is constructed based on the molecular composition in Table 3, in such a way that its size in the x and y direction is consistent with the asphalt model,
2. the layer is added to the asphalt in the z direction (Fig. 4a),
3. a symmetric copy of the system is generated（Fig. 4b),
4. both systems are relaxed for 30 ps in the NPT ensemble (Fig. 4c, Fig. 4d),
5. the two boxes are combined with a 20 Å gap between them representing the micro-crack (Fig. 4f).

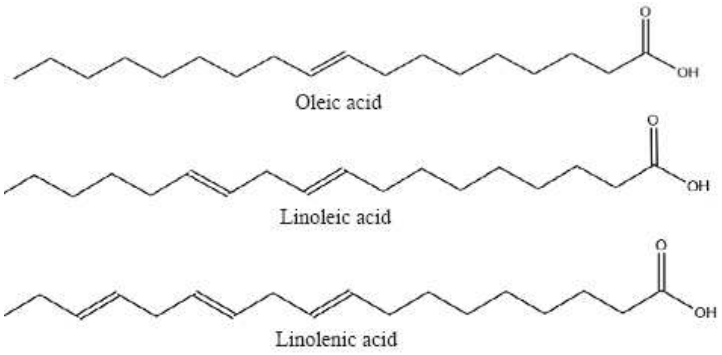

(a) Unsaturated fatty acid

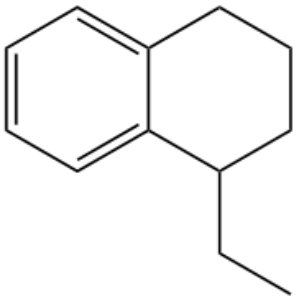

(b) Ethyltetralin

Fig.3. Molecular structures of healing agent model

Table 3 Molecular composition of healing agent model

Healing agent	Molecules	Molecular formula	Molecular weight [Da]	Number of molecules	Fraction Content [%]	Total Molecular weight [Da]
Plant oil	Oleic acid	$C_{18}H_{34}O_2$	282.5	10	40.23	7022
	linoleic acid	$C_{18}H_{32}O_2$	280.5	10	39.95	
	linolenic acid	$C_{18}H_{30}O_2$	278.4	5	19.82	
Aromatic oil	Ethyltetralin	$C_{12}H_{16}$	160.3	44	100	7053.2

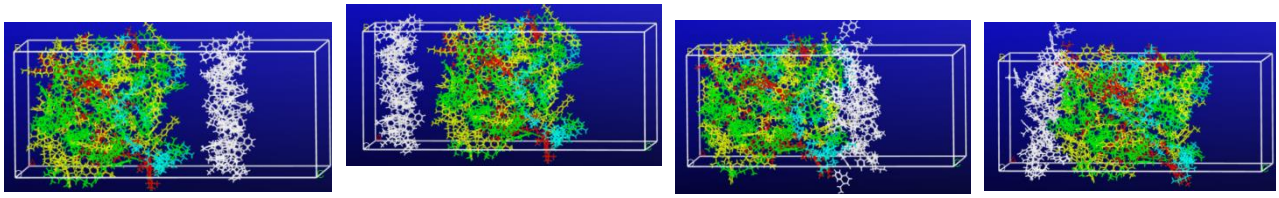

(a) (b) (c) (d)

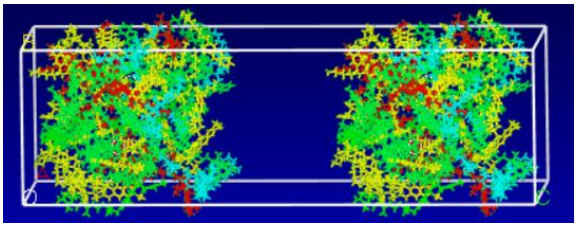

(e)

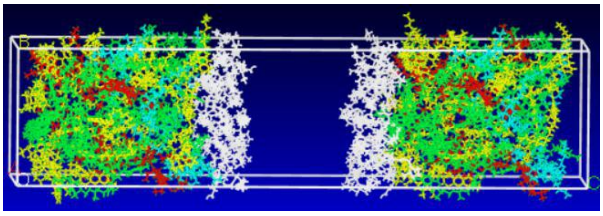

(f)

Fig.4. asphalt micro-crack model: (a) asphalt-healing agent before relaxation; (b) healing agent-asphalt before relaxation: (c) asphalt-healing agent after relaxation; (d) healing agent-asphalt after relaxation; (e) asphalt micro-crack without healing agent; (f) asphalt micro-crack with healing agent (red: Asphaltene, blue: Saturate, yellow: Aromatic, green: Resin, white: healing agent)

2.3 Simulation process and details

The Material Studio (MS) software with the COMPASS II [37] force field is used for the simulations. The time step is 1fs, the cut-off distance 12.5Å, the pressure 1 atm. The Nose-Hoover thermostat is used to control the temperature and the Berendsen barostat to control pressure. Boundary conditions are periodic. Six micro-crack models are investigated: Groups A, B, and C are the virgin-asphalt micro-crack models with, respectively, plant oil, aromatic oil, and no oil. Groups A1, B1, and C1 are the corresponding short-term-aged asphalt models. The simulation methodology is shown in Fig.5.

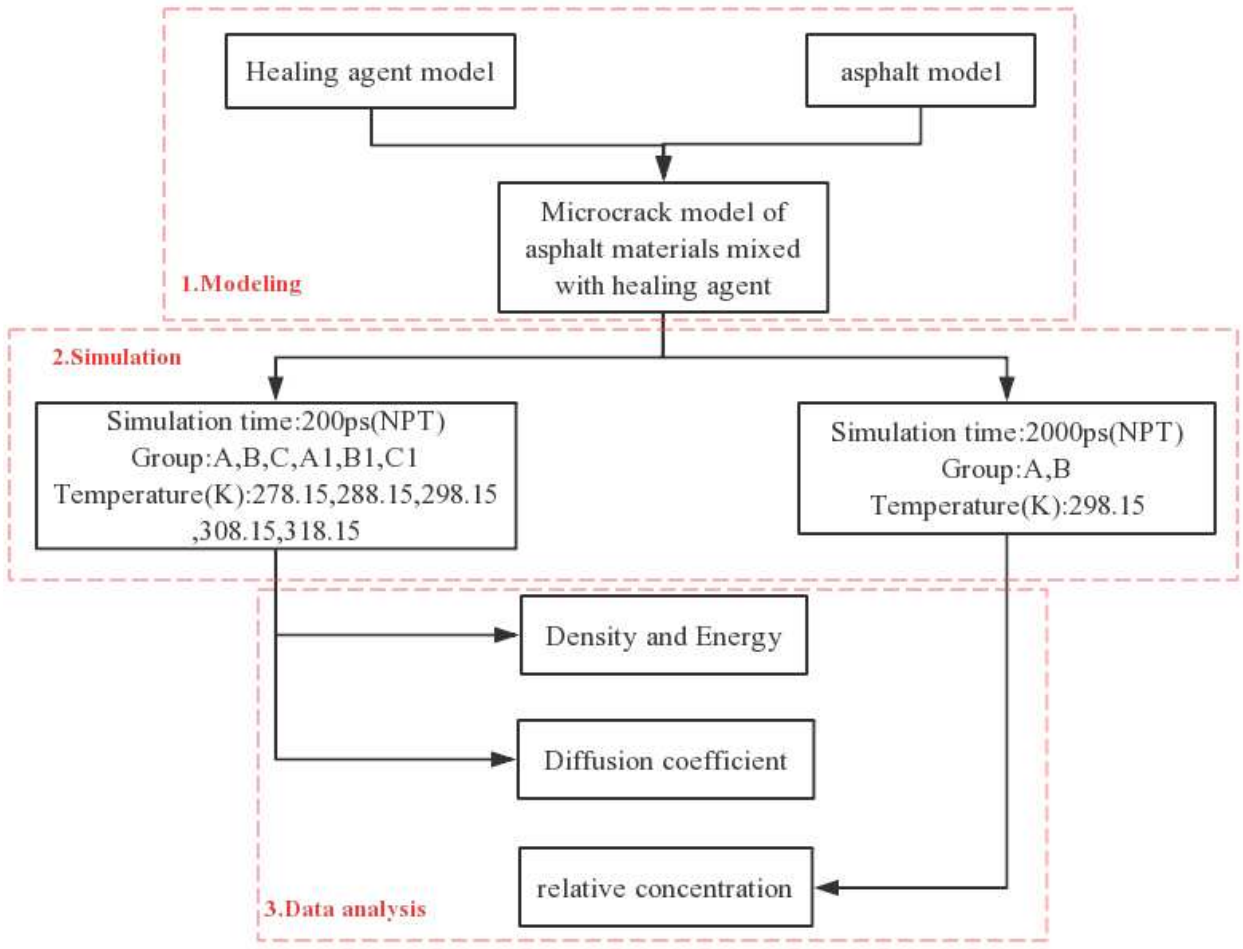

Fig.5. Molecular dynamics simulation process

3 Results and discussion

3.1 Density and Energy analysis

The change in density of the system reflects the healing of asphalt over time. The density curves of group A and group C at 298.15 K are shown in Fig.6. The micro-healing mechanism is due to the diffusion of molecules into the crack. The density of the system increases until the crack is filled. After that, it remains stable. The crack is filled quicker in for group A and B than group C, where there is no healing agent. At 200 ps, the density of group A is 0.977g/cm^3, that of group B is 0.986g/cm^3， and that of group C is 0.987g/cm^3, indicating that the system density with the addition of aromatic oil was similar to that of the virgin asphalt after healing and the addition of plant oil reduces the density of the system.

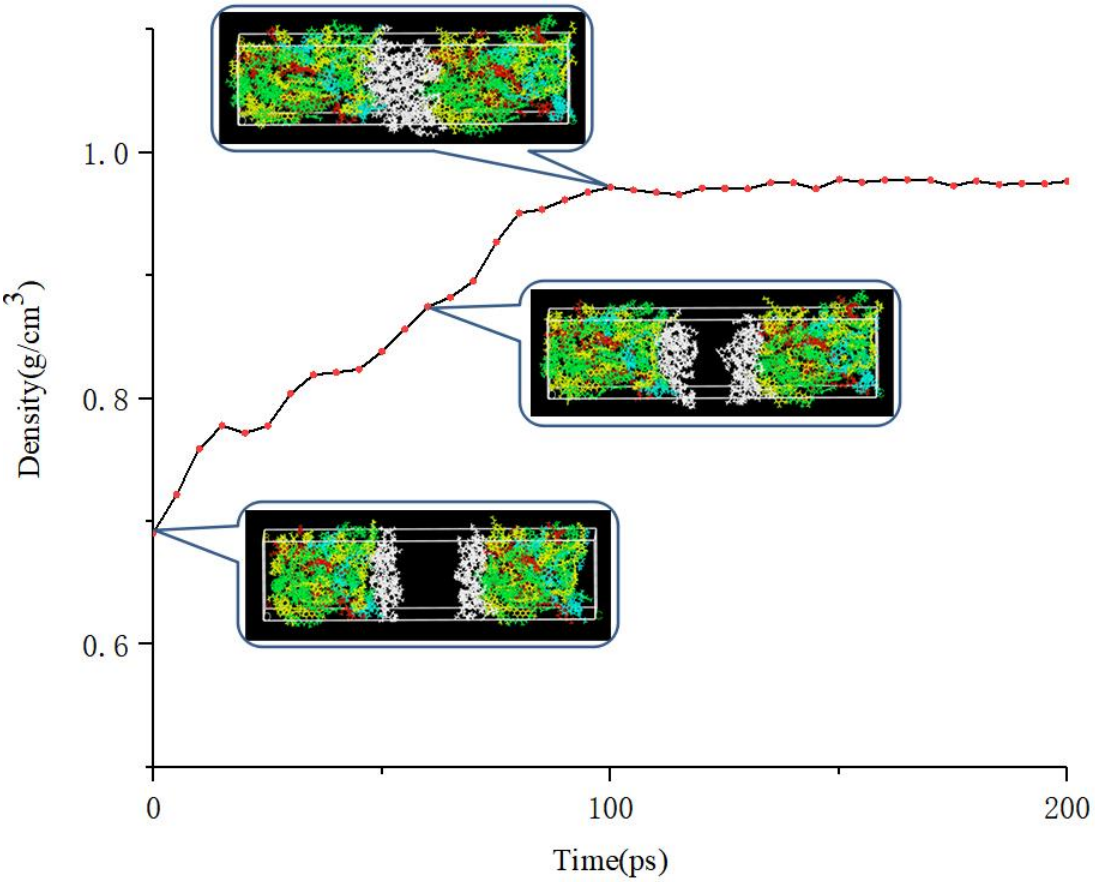

(a) Density curve of group A under 298.15k

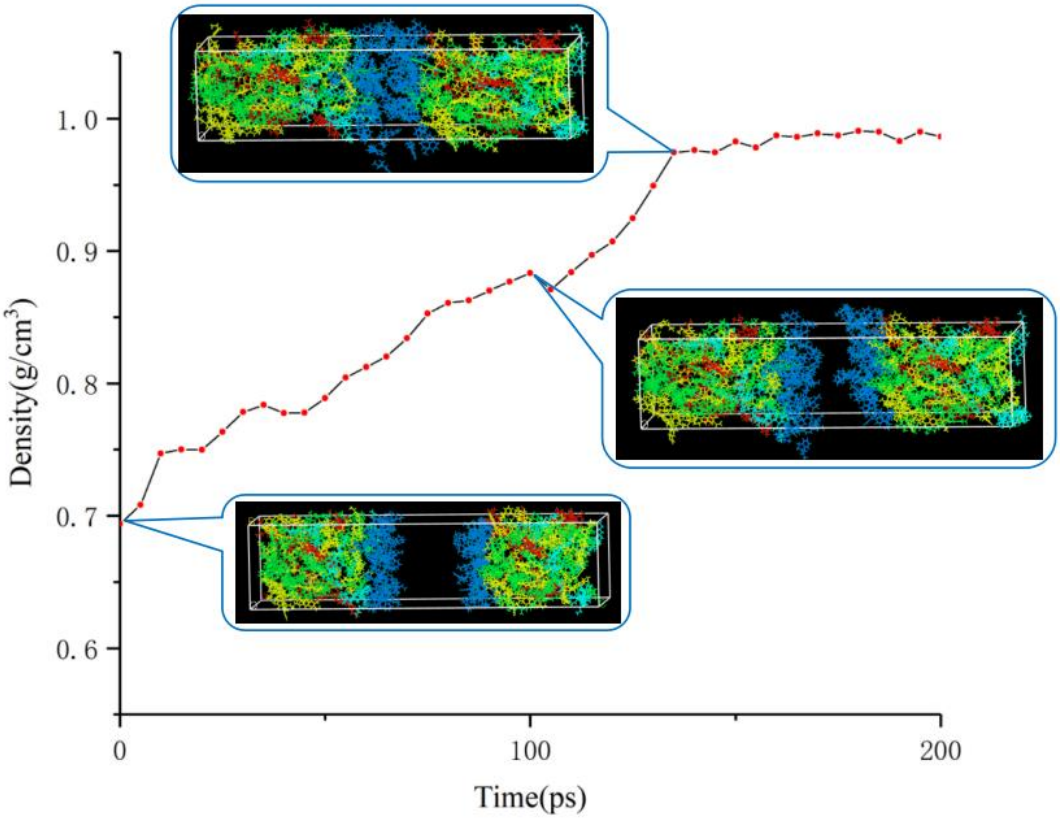

（b） Density curve of group B under 298.15k

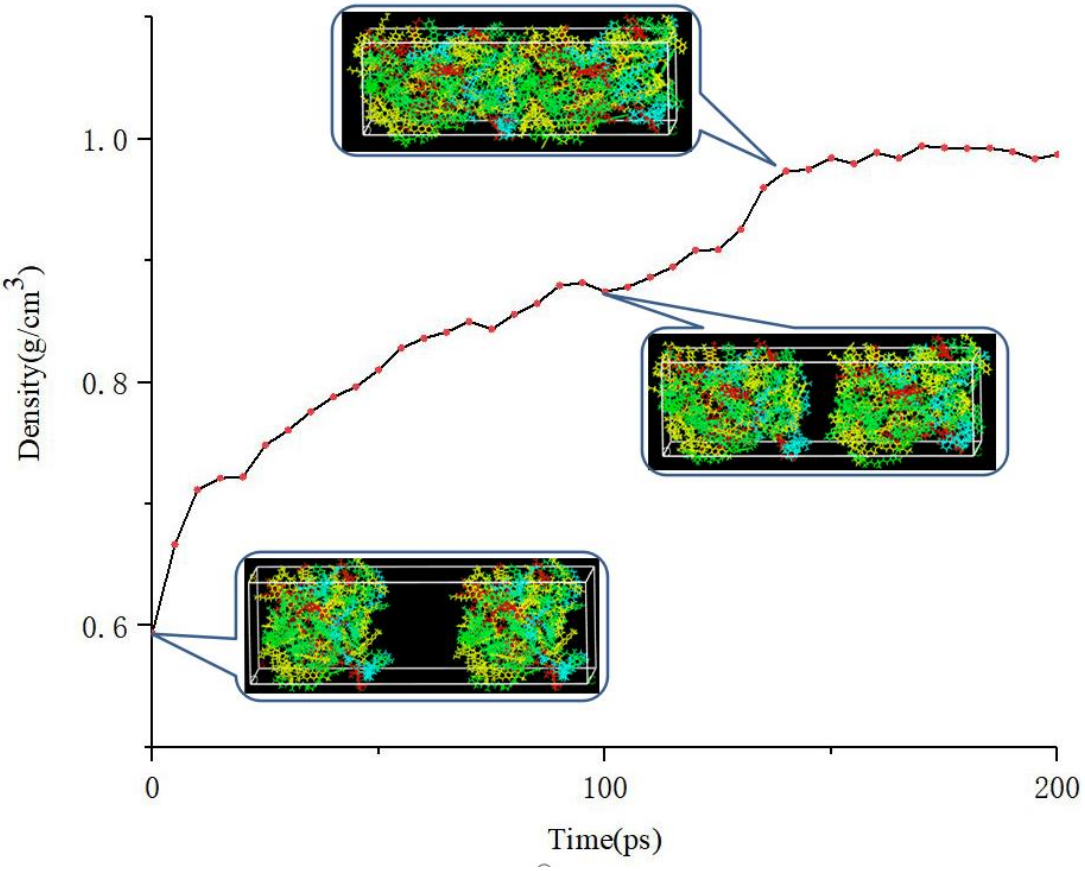

（c） Density curve of group C under 298.15k

Fig.6. Density curve of group A and C under 298.15k (red: Asphaltene, blue: Saturate, yellow: Aromatic, green: Resin, white: Plant oil，Dark blue：Aromatic oil, The blue box shows the conformation of the system at that moment)

The total potential energy of the micro-crack model is equal to the sum of non-bond energy and bond energy. In turn, the non-bond energy is equal to the sum of electrostatic energy, Van der Waals energy, and hydrogen bond energy. Hydrogen bonding contributes very little to the potential energy, so it is not considered. During self-healing, the potential energy decreases as shown in Fig.7. At 5ps, the bond energy decreases sharply probably due to the relaxation of the system. The micro-crack disappears between 5 to 100ps. The van der Waals energy decreases, while the electrostatic and bond energy changes very little. After 100ps, the crack disappears completely, and the potential energy remains approximately constant. This suggests that the diffusion process is mainly driven by Van der Waals forces.

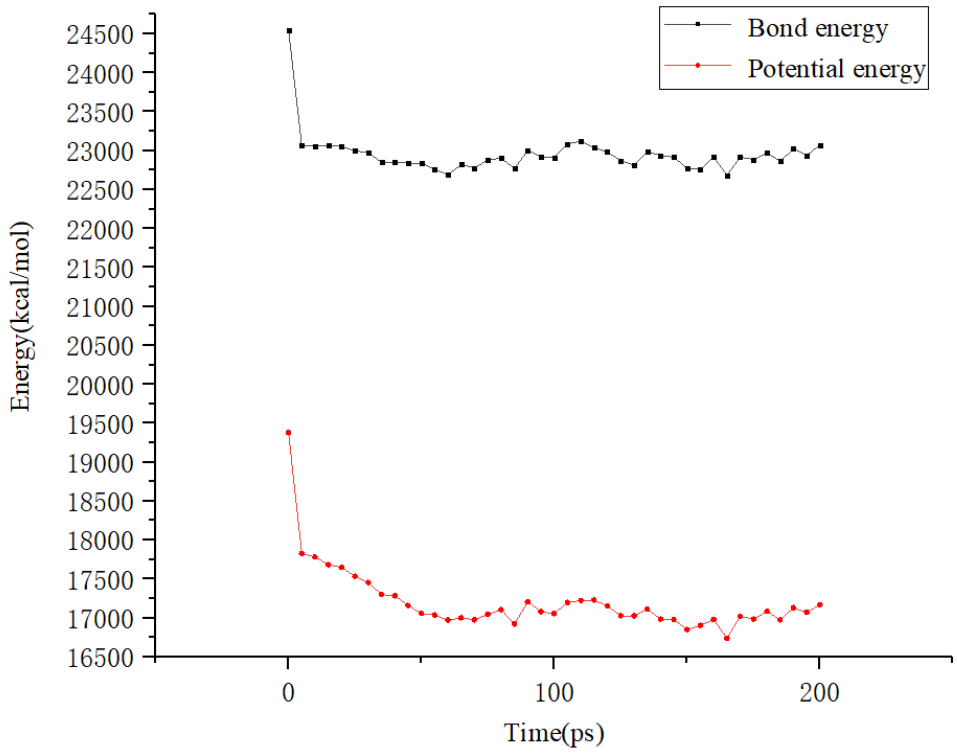

(a) Bond energy and potential energy

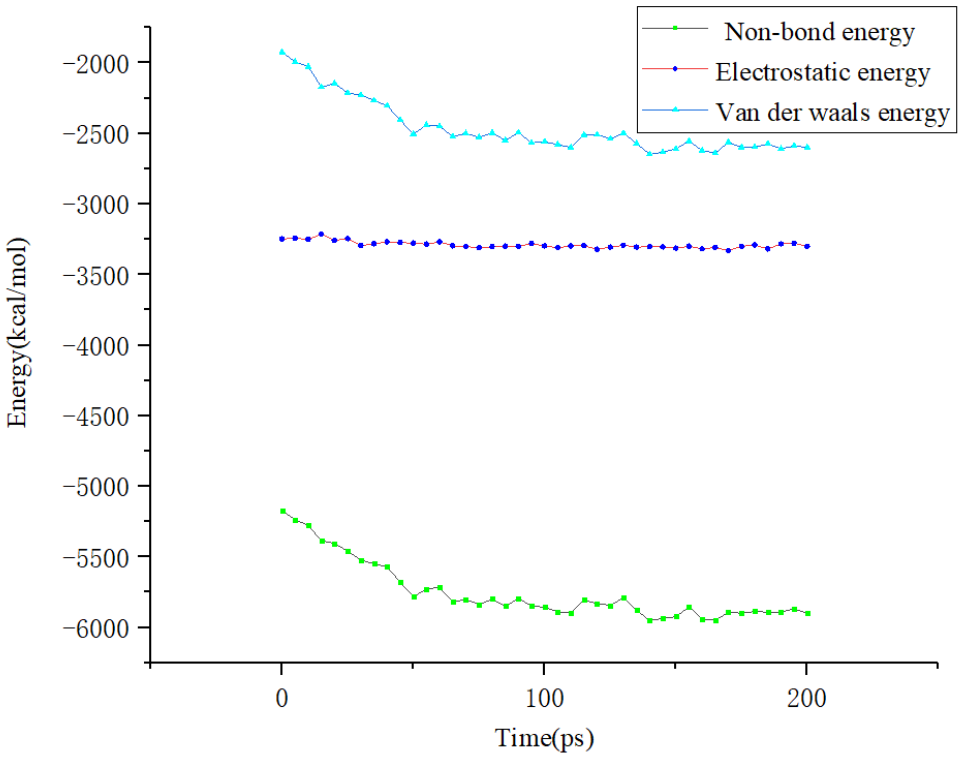

(b) Non-bond energy

Fig.7. Total potential energy of group A under 298.15K

3.2 MSD and diffusion coefficient

During self-healing, molecules of asphalt and healing agents diffuse into the gap of the micro-crack. The faster the molecular diffusion, the faster the healing rate. In this section, the diffusion coefficient is calculated and compared for each group at different temperatures. The diffusion coefficient is calculated from the slope of the MSD. Fig 8 shows the linear fitting for group A at 298.15 K. The calculated diffusion coefficients for all groups are shown in Fig.9.

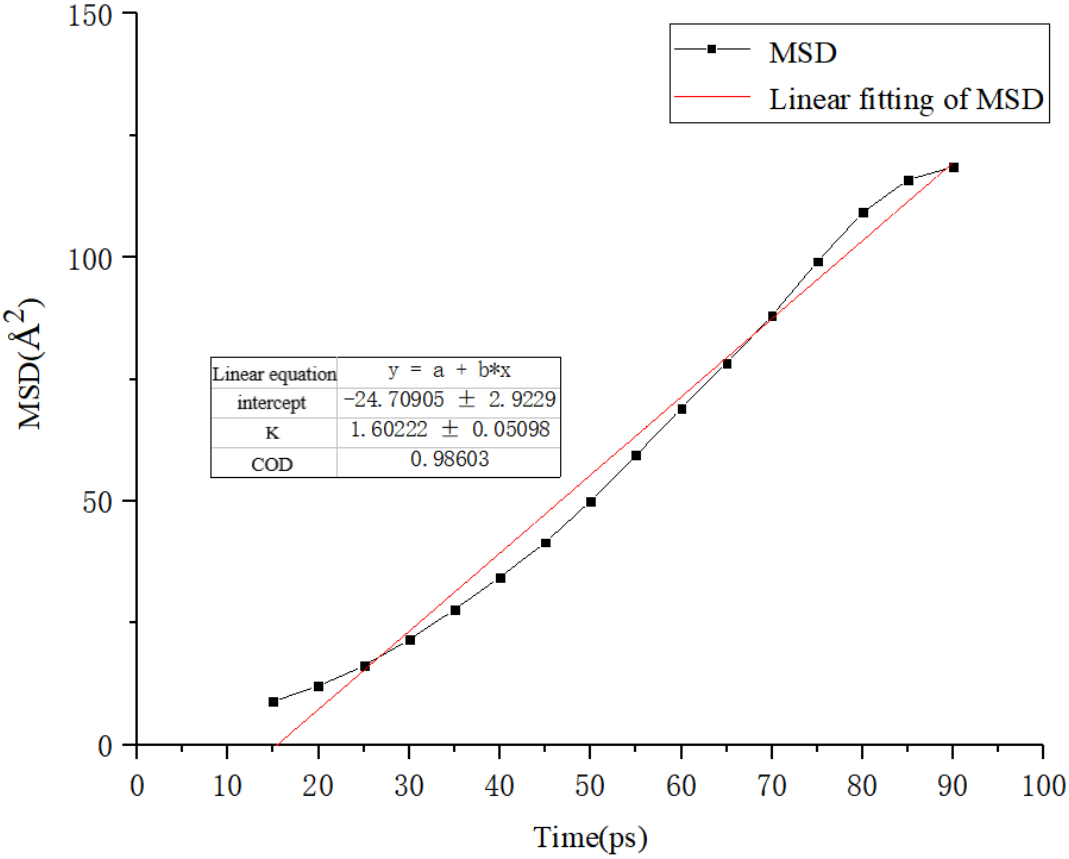

Fig.8. Linear fitting of group A MSD under 298.15K

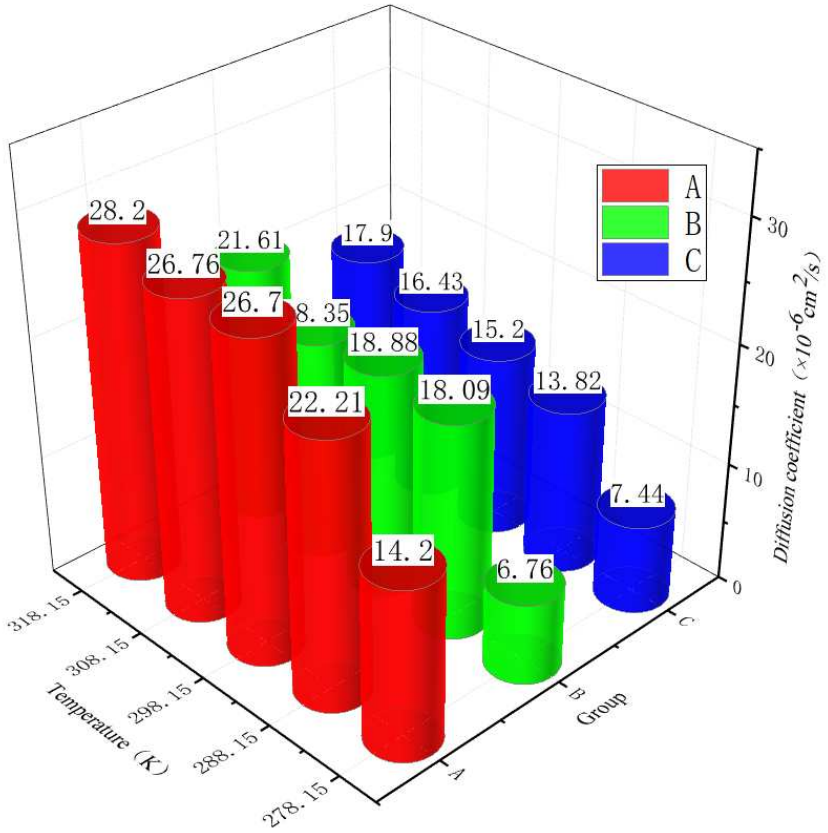

(a) Diffusion coefficient of virgin asphalt during the diffusion process

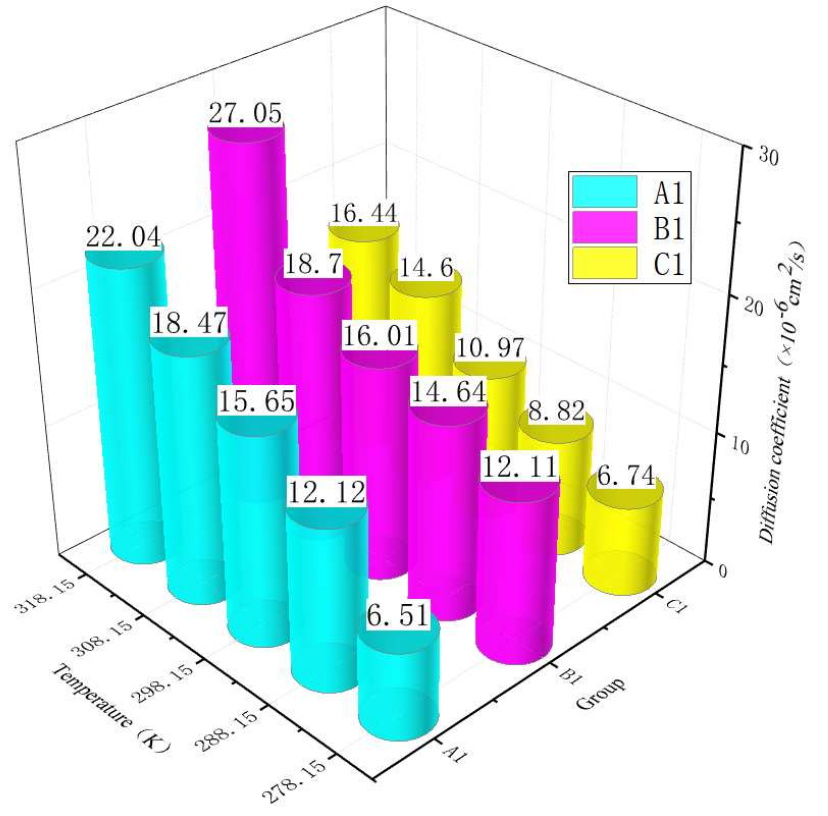

(b) Diffusion coefficient of short-term aged asphalt during the diffusion process

Fig.9. Diffusion coefficient of virgin and short-term aged asphalt during the diffusion process

Figure 9 shows the diffusion coefficients of each group at different temperatures. The diffusion coefficient of virgin asphalt in group A is higher than that of group B, and group B is higher than group C. The diffusion coefficient B1 of short-term aged asphalt is the highest, followed by A1, and C1. Figure 9 also shows that the higher the temperature is, the higher the effect of the healing agent. In particular, healing is faster for temperatures above 15 □ for virgin-asphalt and above 45 □ for short-term-aged asphalt.

Figure 10 shows the diffusivity coefficients of different groups of asphalt at a temperature of 298.15 K. As for virgin asphalt, the addition of a healing agent increases the diffusivity of Resin-A and Aromatic-A more than that of other molecules. It can be seen that the diffusion rate of asphalt molecules has been improved to varying degrees with the addition of healing agents.

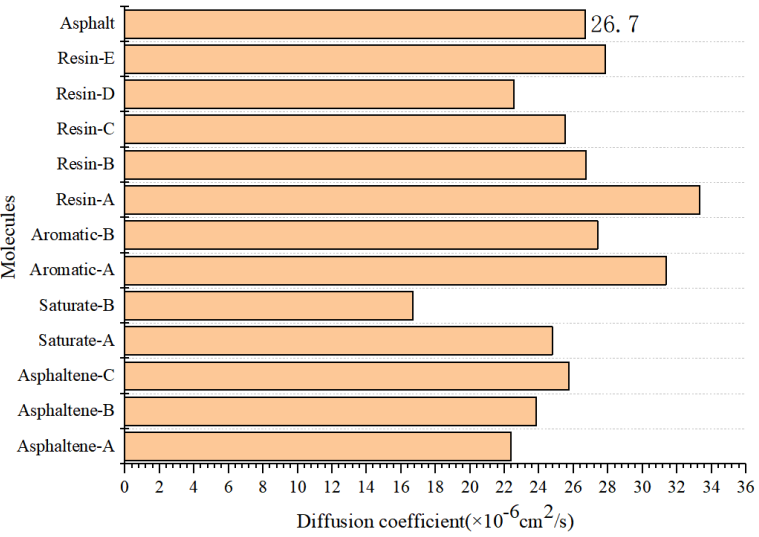

(a) Diffusion coefficient of group A molecules

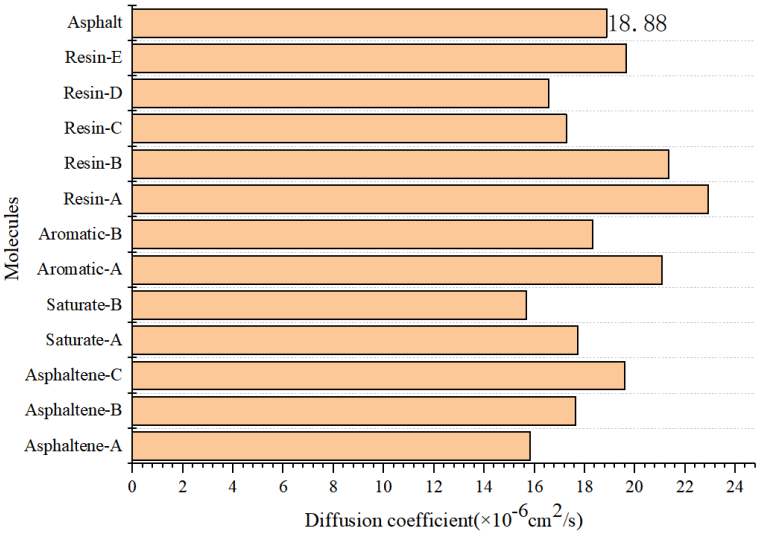

(b) Diffusion coefficient of group B molecules

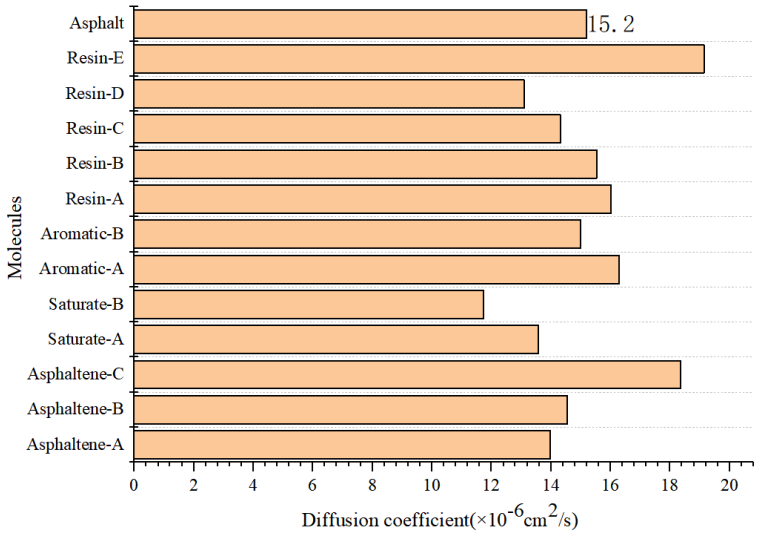

(c) Diffusion coefficient of group C molecules

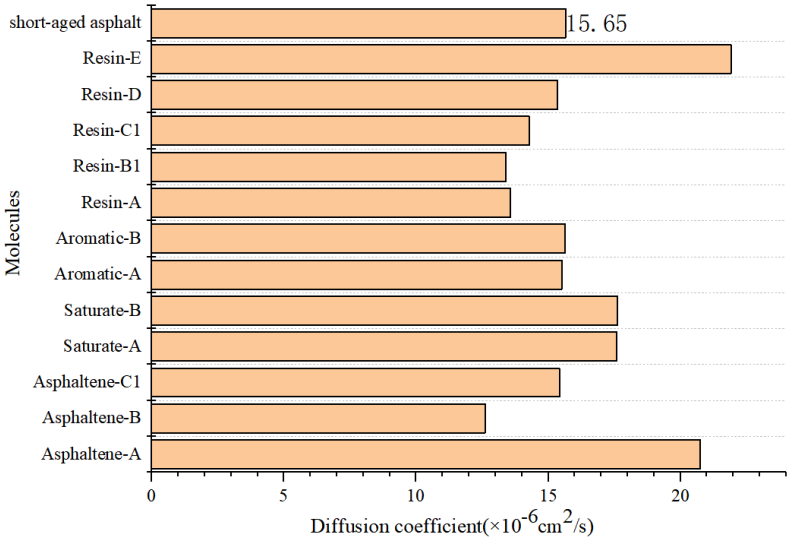

(d) Diffusion coefficient of group A1 molecules

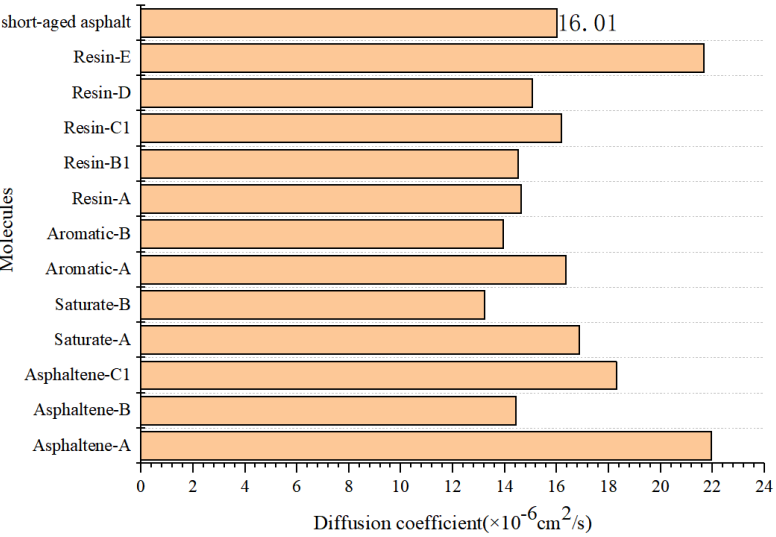

(e) Diffusion coefficient of group B1 molecules

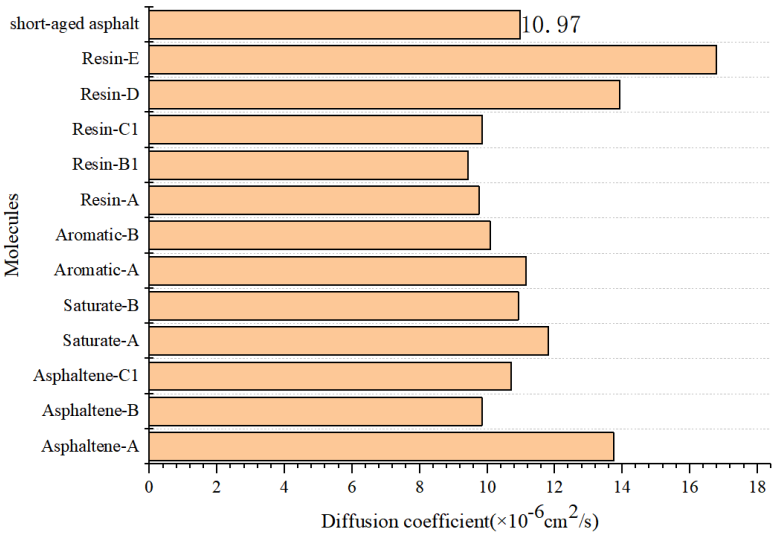

(f) Diffusion coefficient of group C1 molecules

Fig.10. Diffusion coefficient of group A, B, C, A1, B1, C1 molecules

3.3 Relative concentration analysis

During self-healing, the healing agents and asphalt molecules gradually close the gap formed by the micro-crack. Healing occurs when the micro-crack disappears, but molecular motion continues. To understand how healing-agent molecules at the crack surface mix with the surrounding asphalt molecules, the system is simulated in the NPT ensemble at 298.15 K for 2000ps. The relative concentration is defined as

$$C_l = \frac{n_l / V_l}{n_{\text{sample}} / V_{\text{sample}}} \tag{4}$$

where n_l is the number of asphalt atoms in layer l, n_{sample} the number of molecules in the whole sample, V_l is the volume of layer l, V_{sample} the volume of the whole sample.

The relative concentrations of asphalt in groups A and B are shown in Fig.11(a)(b). The relative concentration of asphalt in group A does not change significantly at 100ps, 1000ps, and 2000ps. In group B, it is observed that the relative concentration of asphalt on both sides of the model decreases, while the relative concentration of asphalt in the middle slowly increases. Moreover, there are more zones with a negligible concentration of asphalt in group A than in group B. Fig.12 shows the conformation of the system in groups A and B at 2000ps. It can be observed that there are green resin molecules within the white healing agent molecule in fig.12(b), which indicates that the mixing effect of the healing agent and asphalt molecule in group B is better than that in group A.

Since the size of the box shrinks in the NPT ensemble, the position of the initial micro-crack changes with the size of the box. The position of the micro-crack in this work is from z=a-10(Å) to z=a+10(Å), where “a” is half of the size of the box in the direction of OZ. Fig.13 shows the relative concentration of asphalt in groups A and B at the micro-crack. From 0 to 300ps, the relative concentration of asphalt in group A at the micro-crack is larger than that in group B, and the relative concentration of asphalt in group B is larger than that in group A after 300ps. This indicated that after the completion of self-healing, the mixing effect of the healing-agent and asphalt molecules in group B is better than that in group A， which, in turn, indicates that the asphalt formed after healing of group B is more uniform.

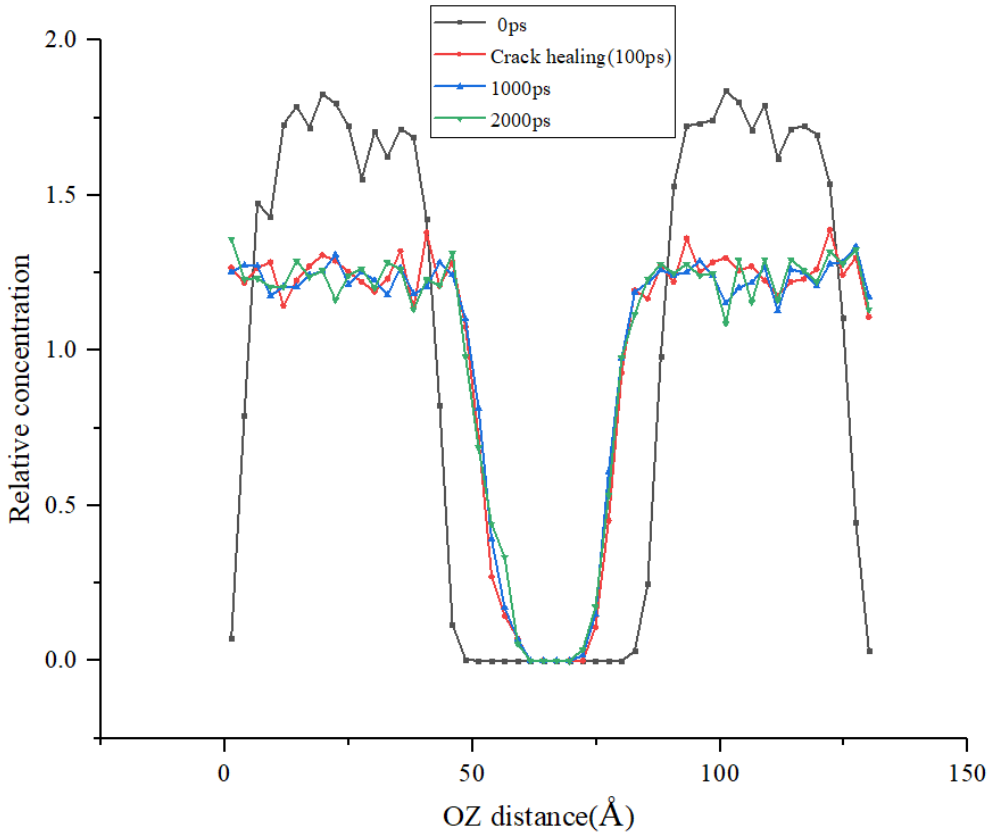

(a) The relative concentration of group A asphalt molecules

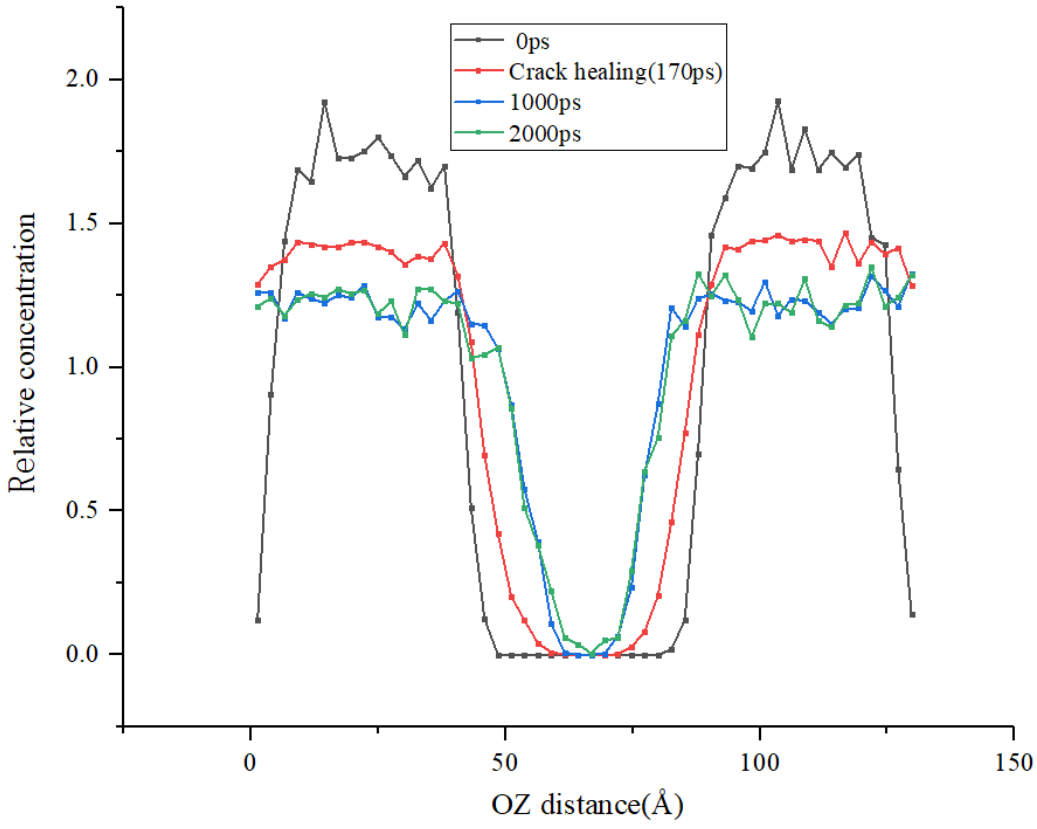

(b) The relative concentration of group B asphalt molecules

Fig.11. The relative concentration of group A and B asphalt under 298.15K

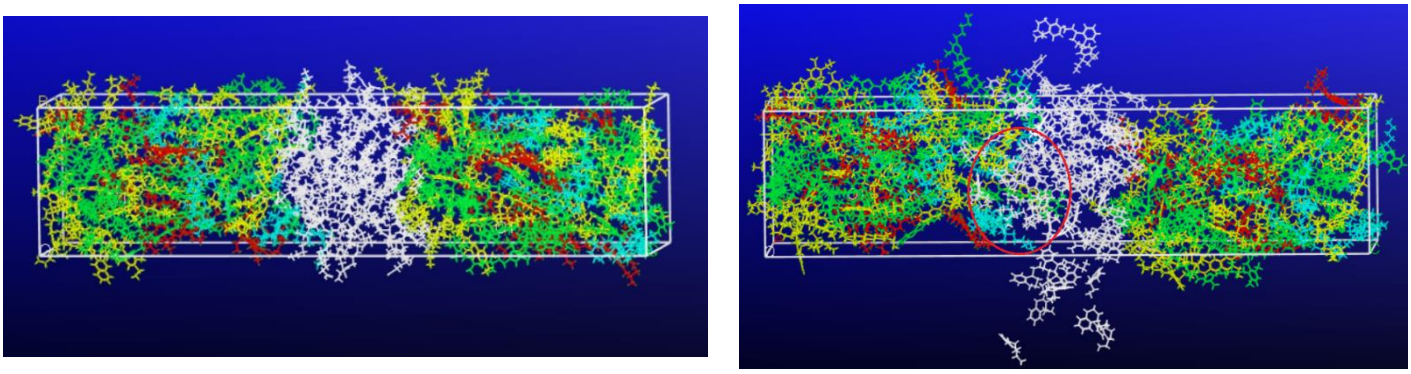

(a) The conformation of group A at 2000ps (b) The conformation of group B at 2000ps

Fig.12. The conformation of group A and B at 2000ps

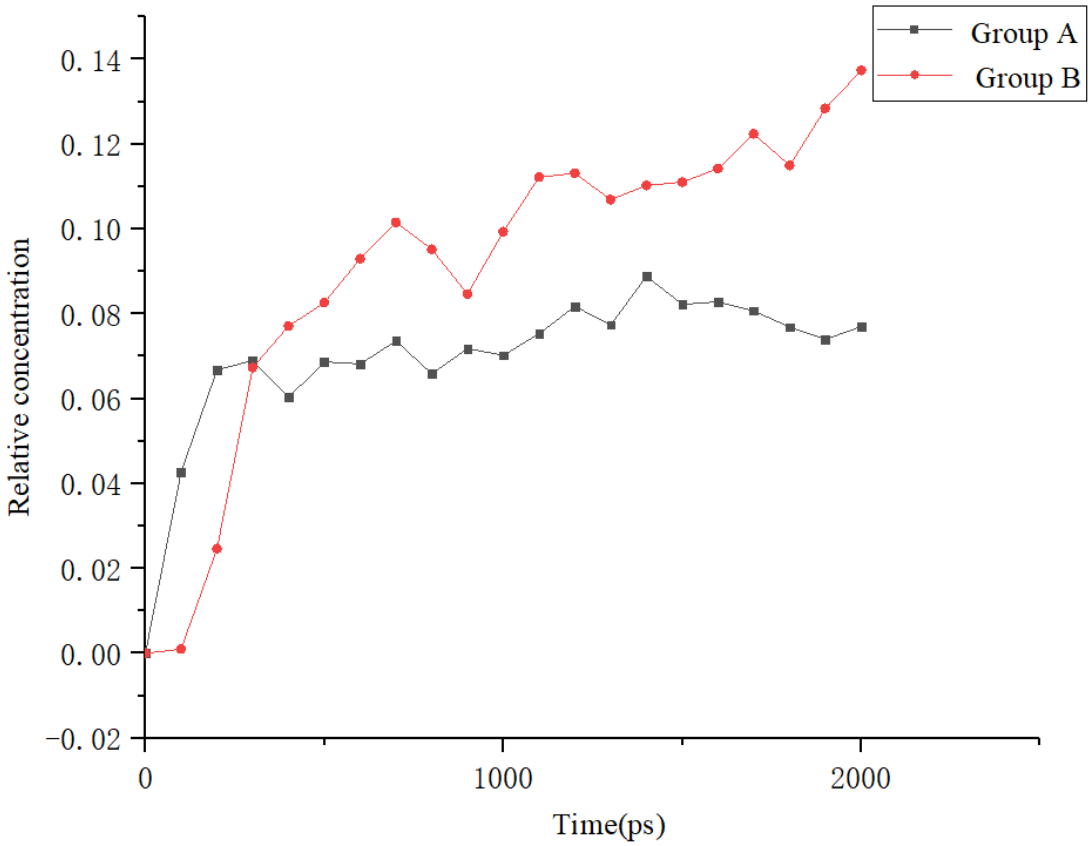

Fig.13. The relative concentration of asphalt molecules in groups A and B at the micro-crack

4 Conclusions

In this paper, a virgin-asphalt model and a short-term-aged asphalt model are set up. The short-term-aged asphalt is obtained by changing the molecular structure and the content of the virgin-asphalt. The asphalt and the healing-agent are combined, and the micro-crack is simulated by a 20Å empty layer. Self-healing is investigated at the molecular level by MD. Changes in density, energy, diffusion coefficient, and relative concentration of the binders are analyzed. The main conclusions are as follows:

(1) Whether it is plant oil or aromatic oil, blending into virgin-asphalt or short-term-aged asphalt binder can improve the healing rate. This improves the self-healing performance of asphalt and plays a positive role in prolonging the life of asphalt pavement.

(2) At the initial stage when the asphalt pavement is put into use with the healing agent, the asphalt has not aged, and the plant oil to the improvement of asphalt healing ability is better than that of aromatic oil healing agents. After short-term aging of asphalt, aromatic oil of asphalt healing ability is superior to the improvement of plant oils healing agent.

(3) The higher the temperature, the better the effect of the healing agent on improving the healing ability of asphalt. The ideal temperatures for the healing agent to improve the healing ability of virgin asphalt and short-term aged asphalt are above 15□ and above 45□, respectively.

(4) The healing agent can improve the diffusion rate of almost all the molecules in the asphalt binder, especially Resin-A and Aromatic-A for virgin asphalt.

(5) After healing, the region where the micro-crack was located has a lower concentration of asphalt mixed with the plant oil. However, the asphalt mixed with the aromatic oil has a more uniform concentration of asphalt, which indicates better mechanical properties.

This study provides a better understanding of the process of asphalt self-healing. It provides a guide for the selection of the more effective healing agents according to the asphalt type and expected operating temperature. It also shows that different asphalt components react differently to the healing agent. This opens the door to a new approach for designing durable asphalts. In the future, for instance, it could be possible to fine-tune asphalt composition to maximize self-healing.

Acknowledgment

This work was supported by Royal Society-Newton Mobility Grant(IE150750), Inter-governmental S&T Cooperation Project of China-Poland (37-13), Inter-governmental S&T Cooperation Project of China-Czech Republic (43-9, 8JCH1002), National Natural Science Foundation of China (52111530134, 51978547), General project of Chongqing Natural Science Foundation (cstc2020jcyj-msxmX0431).

Reference

[1]. Bazin P, Saunier JB. Deformability, fatigue and healing properties of asphalt mixes. proceeding of the second international conference on the structural design of asphalt pavements. Ann Arbor, Michigan, USA 1967; 553.

[2]. Zhang L, Liu Q, Li H, Norambuena Contreras J, Wu S, Bao S, Shu B. Synthesis and characterization of multi-cavity Ca-alginate capsules used for self-healing in asphalt mixtures. Construction and Building Materials, 2019, 211: 298-307.

[3]. Garcia A, Schlangen E, Van de ven M. preparation of capsules containing rejuvenators for their use in asphalt concrete. J Hazard Mater, 2010,181(1): 603-611.

[4]. Micaelo R, Almansoori T, Garcia A. Study of the mechanical properties and self-healing ability of asphalt mixture containing calcium-alginate capsules. Construction and Building Materials, 2016,123: 734-744.

[5]. Su J F, Schlangen E, Qiu J. Design and construction of microcapsules containing rejuvenator for asphalt. Power Technol, 2013, 235：563-571.

[6]. Sun DQ, Hu JL, Zhu XY. Size optimization and self-healing evaluation of microcapsules in asphalt binder. Colloid and Polymer Science, 2015, 293(12):3505-3516.

[7]. Zhang L. Physical and mechanical properties of model asphalt systems calculated using molecular simulation. Dissertations These-Gradworks, 2007.

[8]. Li D D, Greenfield M L, Chemical Compositions of Improved Model Asphalt Systems for Molecular Simulations. Fuel, vol. 115, pp. 347-356, 2014.

[9]. Xu GJ, Wang H. Molecular dynamics study of oxidative aging effect on asphalt binder properties. Fuel. 2017，188(1-10).

[10]. Xu GJ, Wang H, Sun W .Molecular dynamics study of rejuvenator effect on RAP binder Diffusion behavior and molecular structure. Construction and Building Materials. 2018.1,158（1046-1054）.

[11]. Xu M, Yi JY, Qi P, et al. Improved Chemical System for Molecular Simulations of asphalt. Energy & fuels, 2019, 33(APR.): 3187-3198.

[12]. Ding Y, Huang B, Xiang S, et al. Use of molecular dynamics to investigate diffusion between virgin and aged asphalt binders. Fuel, 2016, 174:267-273.

[13]. Qu X，Liu Q, Guo M, et al. Study on the effect of aging on physical properties of asphalt binder from a microscale perspective. Construction and Building Materials, 2018, 187(2018)718-729.

[14]. Ding Y, Tang B, Zhang Y, et al. Molecular Dynamics Simulation to Investigate the Influence of SBS on Molecular Agglomeration Behavior of Asphalt. Journal of Materials in Civil Engineering, 2015, 27(8): C4014004.

[15]. Hu, D., Pei, J., Li, R. et al. Using thermodynamic parameters to study self-healing and interface properties of crumb rubber modified asphalt based on molecular dynamics simulation. Front. Struct. Civ. Eng. 14, 109–122 (2020).

[16]. Guo F, Zhang J, Pei J, et al. Study on the Mechanical Properties of Rubber Asphalt by Molecular Dynamics Simulation. Journal of Molecular Modeling, 2019, 25(12):1-8.

[17]. Chen Z. Strength Generation and Failure Mechanism of Foamed Asphalt Cold Recycled Mixture Based on Molecular Simulation. China：Harbin Institute of Technology, 2019 (in Chinese).

[18]. Xu GJ, Wang H. Study of cohesion and adhesion properties of asphalt concrete with molecular dynamics

simulation. Computational Materials Science, 2016, 112:161-169.

[19]. Bhasin A, Bommavaram R, Greenfield M L, et al. Use of Molecular Dynamics to self-Healing Mechanisms in Asphalt Binders. Journal of Materials in Civil Engineering, 2011, 23(4): 485-492.

[20]. Sun DQ, Lin T, Zhu XY, et al. Indices for Self-healing performance assessments based on molecular dynamics simulation of asphalt binders. Computational Materials Science, 2016, 114: 86-93.

[21]. Sun DQ, Lu T, Zhu XY, et al. Optimization of synthesis technology to improve the design of asphalt self-healing microcapsules. Construction and Building Materials, 2018,175：88-103.

[22]. Xu GJ. Characterization of Asphalt Properties and Asphalt-aggregate Interaction Using Molecular Dynamics simulation. Rutgers：The State University of New Jersey, 2017.

[23]. Petersen, J. C. A dual, sequential mechanism for the oxidation of petroleum asphalts. Pet. Sci. Technol. 1998, 16, 1023− 1059.

[24]. Petersen, J. C.; Dorrence, S. M.; Nazir, M.; et al. Oxidation of Sulfur Compounds in Petroleum Residues: Reactivity-Structural Relationships. Am. Chem. Soc., Div. Pet. Chem., Prepr. 1981, 26:4, 11.

[25]. Petersen, J. C.; Barbour, F. A.; Dorrence, S. M. Identification of dicarboxylic anhydrides in oxidized asphalts. Anal. Chem. 1975, 47, 107− 111.

[26]. Petersen, J. C.; Plancher, H. Quantitative determination of carboxylic acids and their salts and anhydrides in asphalts by selective chemical reactions and differential infrared spectrometry. Anal. Chem. 1981, 53, 786-789.

[27]. Petersen, J. C. Quantitative Functional Group Analysis of Asphalts Using Differential Infrared Spectrometry and Selective Chemical Reactions-Theory and Applications. National Research Council: Washington DC, 1986.

[28]. Cheng YF, Wang C. Oxidative Aging Effects on Damage-Healing Performance of Unmodified and Polymer Modified Asphalt Binders. The 5th International Symposium on Asphalt Pavements & Environment (APE), 2019, pp: 395-403.

[29]. Shahriar A, Zahid H. Changes in Chemical Fingerprints of Asphalt Binders Due to Aging. Testing and Characterization of Asphalt Materials and Pavement Structures. 2018, pp: 44-54.

[30]. Ma T. Research on Hot In-place Recycling Technology of SMA Pavement. China：Southeast University，2010 (in Chinese).

[31]. Greenfield M L. Markoff Random Processes and the Statistical Mechanics of Time-Dependent Phenomenon. □. Irreversible Processes in Fluids. The Journal of Chemical Physics, Vol.22, No.3, pp. 398-413, 1954.

[32]. Andrews A, Guerra R, Mullins O, Sen P. Diffusivity of Asphaltene Molecules by Fluorescence Correlation Spectroscopy. The Journal of Physical Chemistry A, 2006, vol. 110: 8093- 8097.

[33]. Read J, Whiteoak D. The shell bitumen handbook. 5th ed. London, United Kingdom: Thomas Telford Ltd.; 2003.

[34]. Wang P, Dong Z, Tan Y, Liu Z. Investigating the Interactions of the Saturate, Aromatic, Resin, and Asphaltene Four Fractions in Asphalt Binders by Molecular Simulations. Energy and Fuels, vol. 29, pp. 112-121, 2015.

[35]. Painter P C. The Characterization of Asphalt and Asphalt Recyclability. Washington, DC: Strategic Highway Research Program, 1993:1-5.

[36]. Jiang B，Hu WZ，Liu CJ，Chen HY，et al. Comparison of fatty acid composition in nine kinds of vegetable oils. Science and Technology of Food Industry, vol. 8, pp: 108-113, 2015 (in Chinese).

[37]. Sun H, Jin Z, Yang C, et al. COMPASS II: extended coverage for polymer and drug-like molecule databases. Journal of Molecular Modeling, 22(2):47, 2016.